

Y. Murakami* and M. Endo†

Effects of Hardness and Crack Geometries on ΔK_{th} of Small Cracks Emanating from Small Defects

REFERENCE Murakami, Y. and Endo, M. Effects of Hardness and Crack Geometries on ΔK_{th} of Small Cracks Emanating from Small Defects, *The Behaviour of Short Fatigue Cracks*, EGF Pub. 1 (Edited by K. J. Miller and E. R. de los Rios) 1986, Mechanical Engineering Publications, London, pp. 275–293.

ABSTRACT The dependence of ΔK_{th} on crack size and material properties at a stress ratio $R = -1$ was studied on various materials and microstructures. The values of ΔK_{th} of all materials investigated were unified with one geometrical and one material parameter.

The geometrical parameter is the square root of the area determined by projecting defects or cracks onto the plane normal to the maximum tensile stress. The relationship

$$\Delta K_{th} \propto (\sqrt{area})^{1/3}$$

is derived.

The most relevant material parameter to unify data is the Vickers hardness and the relationship

$$\Delta K_{th} \propto (H_v + C)$$

is obtained. The constant C reflects the difference of non-propagation behaviour of small cracks in soft and hard metals.

Combining these equations, experiments show that ΔK_{th} and the fatigue limit σ_w of cracked members are given by

$$\Delta K_{th} = 3.3 \times 10^{-3} (H_v + 120) (\sqrt{area})^{1/3}$$

and

$$\sigma_w = 1.43 (H_v + 120) / (\sqrt{area})^{1/6}$$

Here ΔK_{th} is in $\text{MPa}\sqrt{\text{m}}$, \sqrt{area} in μm , and σ_w in MPa. These equations are applicable to cracks having \sqrt{area} approximately less than $1000 \mu\text{m}$.

Notation

<i>area</i>	The area which is occupied by projecting a defect or a crack onto the plane normal to the maximum tensile stress
α, C, C_1, C_2, n	Constants independent of material
C', n'	Constants dependent on material
H_B	The Brinell hardness number (BHN)
H_v	The Vickers hardness number (DPH)
K_I	Stress intensity factor (mode I)
$K_{I\max}$	The maximum value of the stress intensity factor along the front of a three-dimensional crack (mode I)

* Department of Mechanics and Strength of Solids, Faculty of Engineering, Kyushu University, Higashi-ku, Fukuoka, 812 Japan

† Department of Mechanical Engineering, Fukuoka University, Jonan-ku, Fukuoka, 814-01 Japan

ΔK_{th}	Threshold stress intensity factor range ($R = -1$)
ΔK_{eff}	Effective stress intensity factor range
$\Delta K_{eff,th}$	Threshold effective stress intensity factor range
l	Length of a two-dimensional crack
l_f	Fictitious crack length
l_0	The maximum length of a non-propagating crack observed in unnotched specimens at the fatigue limit
ν	Poisson's ratio
R	Stress ratio
σ_U	Ultimate tensile strength
σ_w	Fatigue limit
σ_{w_0}	Fatigue limit of an unnotched specimen
σ_Y	Yield stress
σ_0	The maximum tensile stress

Introduction

The threshold stress intensity factor range ΔK_{th} is required in order to determine the maximum allowable stress when cracks or defects are detected in machine parts and structures under service loading. However, recent experimental studies (1)–(6) show that the value of ΔK_{th} is dependent on crack size, i.e., the smaller the crack, the smaller the value of ΔK_{th} . On the other hand, the value of ΔK_{eff} characterizes the growth behaviour of not only a large crack but also a small one, and, accordingly, $\Delta K_{eff,th}$ is almost independent of crack size (7)(8). However, in practice, the application of ΔK_{eff} or $\Delta K_{eff,th}$ is inconvenient, because we must measure or assume the opening ratio of a crack in real structures, and this measurement is very difficult. Therefore, it is preferable in practice to determine the value of ΔK_{th} as a function of crack size and geometry and then to estimate the allowable stress from ΔK_{th} rather than to measure ΔK_{eff} .

The correlation between the fatigue limit σ_w and the crack length l was first obtained by Frost (9). But at the time when Frost carried out his fatigue tests and obtained the relationship $\sigma_w^2 l = \text{constant}$, the fatigue threshold phenomena and the dependence of ΔK_{th} on crack length were not recognized.

Kitagawa and Takahashi (3) pointed out that ΔK_{th} decreases with decreasing crack size. However, an expression for ΔK_{th} as a function of crack size was not given explicitly. El Haddad *et al.* (10) added the fictitious crack length l_f to the real crack length l in order to compensate for the decreasing value of ΔK_{th} with decreasing crack length. The value of l_f , considered to be a material constant, was determined from ΔK_{th} for a large crack, and from the fatigue limit of an unnotched specimen, σ_{w_0} . However, the physical meaning of l_f and the rule for determining l_f for various three-dimensional cracks are not clear.

In many previous studies, comparison of ΔK_{th} values for different materials did not consider the dependence of ΔK_{th} on crack size and geometry. Such

comparisons are likely to induce erroneous conclusions. One objective of the present paper is to elucidate the dependence of ΔK_{th} on the shape and size of cracks with special emphasis on small cracks. The large amount of available data on rotating bending fatigue in various materials is analysed. A geometrical parameter $\sqrt{\text{area}}$, which is defined by the square root of the projection area of defects or cracks onto the plane perpendicular to the maximum tensile stress, is proposed in order to unify the effects of various notches, holes, and cracks. An explicit relationship between ΔK_{th} and $\sqrt{\text{area}}$ is confirmed for more than ten materials.

Another objective is to find the most appropriate material parameter which reflects the threshold behaviour. It should be noted that the dependence of ΔK_{th} on material parameters can be made clear only after the most appropriate geometrical parameter is found. Although various material parameters such as yield stress (σ_Y), ultimate tensile stress (σ_U) and hardness (H_v or H_B), may be correlated with ΔK_{th} , the Vickers hardness number H_v was chosen after observing the trend of many data and also for the reasons of simplicity of measurement and availability.

Finally, a simple formula for predicting ΔK_{th} in terms of one material and one geometrical parameter, i.e., H_v and $\sqrt{\text{area}}$, is derived.

A geometrical parameter for small defects or cracks

Effects of small defects, cracks, and inclusions on fatigue strength have been investigated by many researchers (11)–(19). However, their effects are so complicated that no method for unifying them quantitatively has been established. The crucial cause for the absence of a unifying method was an incorrect understanding of the threshold condition for such small defects, cracks, and inclusions. Murakami and Endo (20) showed how to overcome this difficulty by interpreting the fatigue limit not as the critical condition for crack initiation but as the condition for the non-propagation of a crack emanating from defects, cracks, and inclusions; previously Miller *et al.* (21)(22) had applied a similar consideration to notches. For example, the fatigue limit of a structural component containing a small defect must not be interpreted as a notch problem in which the critical condition of crack initiation is questioned, but should be understood as a problem of a crack which emanates from the defect and stops propagating. Only the interpretation of problems in this manner leads us to find the geometrical parameter for defects, cracks, and even sharp notches. It is reasonable to seek the geometrical parameter from the standpoint that the effects of shapes and sizes of cracks on fatigue strength may be correlated with stress intensity factors, especially with the maximum stress intensity factor along the three-dimensional crack front. Previous studies by Murakami *et al.* (20)(23)–(31) regarding this problem can be summarized as follows.

First, the stress intensity factors, K_I , for elliptical cracks in an infinite body under uniform tension were investigated and the approximate relationship

between the maximum value ($K_{I_{max}}$) at the tip of the minor axis of an ellipse and the crack area was given as follow (20)

$$K_{I_{max}} \propto (\sqrt{area})^{1/2} \quad (1)$$

Afterwards, three-dimensional stress analyses by the body force method were carried out for surface cracks having various shapes, and the maximum value of the stress intensity factor along their crack front was correlated with the crack areas to give the following equation (23)–(25) (see Appendix 2):

$$K_{I_{max}} \cong 0.65 \sigma_0 \sqrt{(\pi \sqrt{area})} \quad (2)$$

The error in equation (2) may be estimated to be less than 10 per cent. Equation (2) implies that the square root of the crack area projected onto the plane perpendicular to the maximum tensile stress should be adopted as the most relevant geometrical parameter for three-dimensional cracks.

When a specimen has a three-dimensional defect other than a planar crack, the fatigue limit is determined by the threshold condition of the crack emanating from the defect (20)(26)–(30). In this case, the initial three-dimensional shape of the defect is not directly correlated with the stress intensity factor. Rather, the planar domain (area) which is occupied by projecting the defect onto the plane perpendicular to the maximum principal stress should be regarded as the equivalent crack and the stress intensity factor should be evaluated from the equivalent crack, see Fig. 1(b). This may be easily understood from a simple two-dimensional example; the stress intensity factor for an elliptical hole having cracks at the ends of the major axis can be approximately estimated from those of an equivalent crack with a total length of (major axis + crack length). Here, it should be noted that the area of crack emanating from a three-dimensional crack occupies only a small portion of the total projected area (28)(31), see Fig. 1(a), and accordingly the area of an equivalent crack

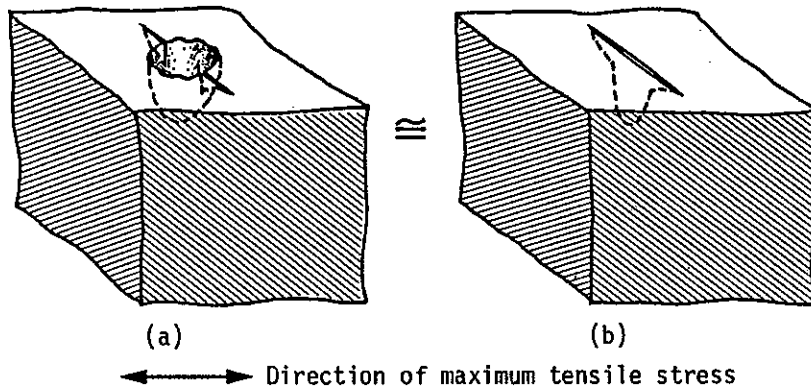


Fig 1 Defect with cracks and its equivalent crack

which should be used for equation (2) may be estimated by the projected area of the initial defect.

From the above discussion, it can be hypothesized that the square root of crack area or the projected area of defects is the relevant geometrical parameter to use when determining quantitatively the fatigue strength of structural components containing various cracks and defects in which no apparent mutual correlations are obvious. With regard to an estimation of \sqrt{area} for irregularly shaped cracks, see Appendix 1.

On the basis of this hypothesis, previous data on rotating bending fatigue were analysed using the parameter \sqrt{area} . The artificial defects investigated in this study are very small drilled holes (20)(28)–(30)(32)–(35) with diameters ranging from 40 μm to 500 μm and depths greater than 40 μm , also very small and shallow notches (35)–(46) with depths ranging from 5 μm to 300 μm , and very shallow circumferential cracks (47) with depths greater than 30 μm , and finally a Vickers hardness indentation (35) of 72 μm surface length. The shapes of defects and cracks considered are shown in Fig. 2. The effects of work hardening and residual stress by introducing the drilled holes were examined and found to be small (20). In those tests almost all notched specimens were electropolished after introducing the notches (35)–(46) and the cracked specimens were annealed after introducing the fatigue cracks (47). Accordingly the effect of work hardening would be expected to be negligible.

The relationship between ΔK_{th} and \sqrt{area} is illustrated in Fig. 3. the data in the figure were adopted from various references as well as previous studies by the authors' group. Although this figure may be similar to that of Kitagawa and Takahashi (3), the parameter of abscissa is not crack length but the new parameter \sqrt{area} which can unify the size effect of three-dimensional defects and cracks. Moreover, the adoption of the new parameter \sqrt{area} characterizes the threshold behaviour particularly for the data on very small cracks.

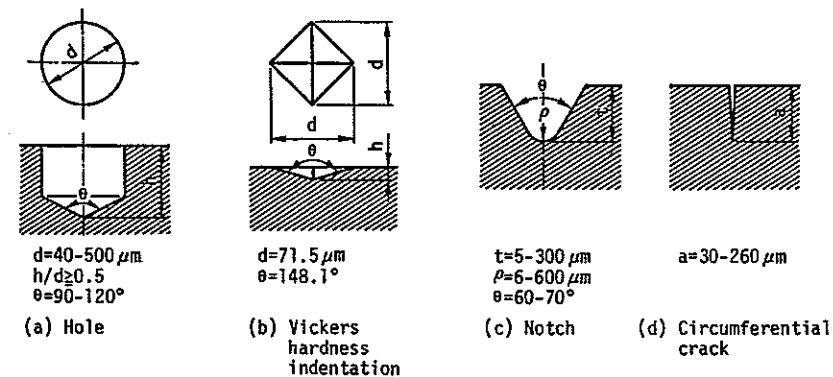


Fig 2 The shapes of defects and cracks investigated in this study

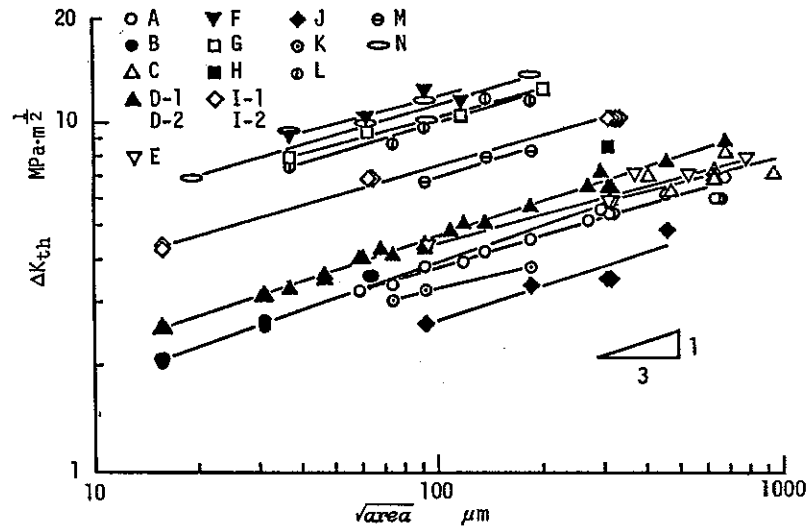


Fig 3 Relationship between ΔK_{th} and \sqrt{area} for various defects and cracks. Letters correspond to the materials given in Table 1

For the region $\sqrt{area} \leq 1000 \mu\text{m}$, the relationship between ΔK_{th} and \sqrt{area} is approximately linear and the following equation holds regardless of material

$$\Delta K_{th} \propto (\sqrt{area})^{1/3} \quad (3)$$

Equation (3) characterizes the distinct dependence of ΔK_{th} on the geometrical parameter \sqrt{area} . Equation (3) implies also that if we investigate ΔK_{th} of specimens containing a very short two-dimensional crack of length l , we have

$$\Delta K_{th} \propto l^{1/3} \quad (4)$$

If we convert the empirical formula obtained by Frost (9), i.e., $\sigma_w^2 l = \text{constant}$, to the same form as equation (4), we have

$$\Delta K_{th} \propto l^{1/6} \quad (5)$$

Equations (4) and (5) contradict each other. This is because the experiments by Frost contain longer or larger cracks than those of the data in Fig. 3. With increasing crack length ΔK_{th} approaches a constant value depending on the specific material. This indicates that the slope of the relationship between ΔK_{th} and \sqrt{area} (or l) on a log-log scale varies from one-third to zero with increasing crack size and, therefore, the slope of one-sixth in equation (5) corresponds to a transient value from one-third to zero. This point was recently discussed in detail by Murakami and Matsuda (48).

Vickers hardness as a representative material parameter

Figure 3 presents data on an aluminum alloy and 70/30 brass in addition to various steels. The Vickers hardness H_v of these materials is shown in Table 1. It ranges over from 70 to 720 covering a range of a factor of ten.

From the tendency of ΔK_{th} in Fig. 3, it may be noted that the materials having higher Vickers hardness show higher values of ΔK_{th} (and accordingly higher fatigue strength). However, the tendency cannot be expressed in a simple form such as $\Delta K_{th} \propto H_v$. It has been empirically observed that the fatigue limit of a specimen containing a notch or a defect is not directly proportional to the Vickers hardness. This is presumably because the occurrence of non-propagating cracks may have a different dependency. In other words, a crack is likely to show non-propagating behaviour in soft materials while, on the contrary, it is difficult to find non-propagating cracks at the fatigue limit of hard steels. With increasing hardness non-propagating cracks are experienced only within a narrow range of stress amplitude, and in this case the length of non-propagating cracks is usually very short. Therefore, it may be concluded that ΔK_{th} is not a function of the form $\Delta K_{th} \propto H_v$ or $\Delta K_{th} \propto H_v^2$. The difference of threshold behaviour between soft and hard materials may rather be expressed by the following formula

$$\Delta K_{th} \propto (H_v + C) \quad (6)$$

where C is a constant independent of materials. In order to check this prediction the values of $\Delta K_{th}/(\sqrt{area})^{1/3}$ were plotted against H_v from consideration of equation (3) and the validity of equation (6) was confirmed by many data with only a few exceptional data on stainless steels. (See Appendix 3). Now considering equations (3) and (6), the following equation is expected to hold for a wide range of materials

$$\Delta K_{th} = C_1(H_v + C_2)(\sqrt{area})^{1/3} \quad (7)$$

where C_1 and C_2 are constants independent of material.

The constants C_1 and C_2 in equation (7) can be determined by the least square method applied to the data in Fig. 3 and we have

$$\Delta K_{th} = 3.3 \times 10^{-3}(H_v + 120)(\sqrt{area})^{1/3} \quad (8)$$

where the units of ΔK_{th} are $\text{MPa}\sqrt{\text{m}}$ and that of \sqrt{area} is μm .

Figure 4 shows the comparison of the experimental data in Fig. 3 and the correlation by equation (8). It is pleasing to note that the various data for H_v ranging from 70 to 720 are well represented by equation (8). The reason why equation (8) is not good in predicting ΔK_{th} for two kinds of stainless steels (34) is presumably because non-propagating cracks are unlikely to be observed in stainless steels even at a sharp notch (49)–(51). The existence of non-propagating cracks in the data of (34) was not checked in the present study.

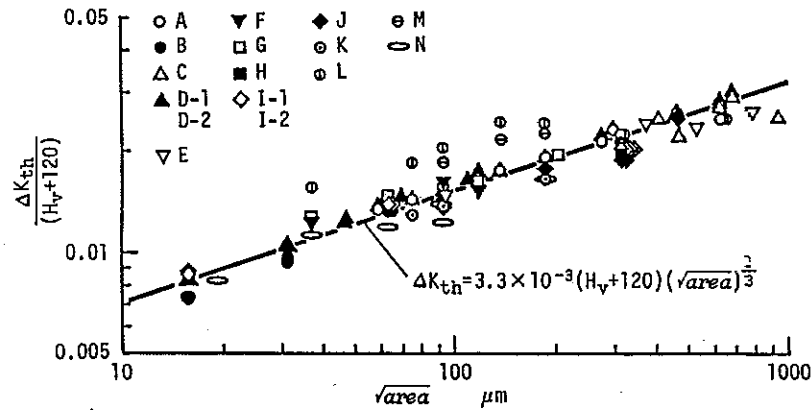


Fig 4 Relationship between $\Delta K_{th}/(H_v + 120)$ and \sqrt{area} . Letters correspond to the materials listed in Table 1

Combining equations (8) and (2), the fatigue limit σ_w of a cracked specimen can be expressed as

$$\sigma_w = 1.43(H_v + 120)/(\sqrt{area})^{1/6} \tag{9}$$

where σ_w is the nominal stress defined for the gross diameter and has units of MPa.

Murakami and Endo (20) previously proposed an equation of the form $\sigma_w \sqrt{area} = C'$ for predicting the fatigue limit of materials containing defects or cracks. Although this equation is very accurate, the negative aspect of it is that we need fatigue tests for individual materials to determine n' and C' (52). This disadvantage is overcome by equations (8) or (9).

Table 1 shows the comparison of the values predicted by equations (8) and (9) with experimental results. For most materials except two kinds of stainless steels, the error is less than 10 per cent.

It should be noted that Fig. 4 and Table 1 include many results of specimens containing an extremely shallow notch (depths ranging from 5 to 20 μm) or a crack, or very small holes (diameters ranging from 40 to 500 μm), and although it may be said that the theory of the notch effect has been established for medium or deep notches, conventional theories (22)(43)(44)(53)–(57) may not be applicable to extremely shallow notches. From the viewpoint of the present study however, extremely shallow notches may be placed in the category of small cracks, and so the prediction of the fatigue limit can be simply made by equations (8) or (9).

Table 1 Comparison of predicted values by equations (8) and (9) with experimental results

Material	Defect	H_v	\sqrt{area} (μm)	ΔK_{th} (MPa $\sqrt{\text{m}}$)		σ_w (MPa)		Error (%)
				Expt	Pred.	Expt	Pred.	
A: S10C (annealed) (36)	Notch	120	632	6.1	6.8	105	117	11.8
A: S10C (annealed) (37)		120	632	6.1	6.8	105	117	11.8
A: S10C (annealed) (38)	Notch	120	316	5.5	5.4	134	132	-1.6
		120	316	5.5	5.4	134	132	-1.6
A: S10C (annealed) (20)(28)	Hole	120	74	3.4	3.3	172	168	-2.5
		120	60	3.2	3.1	181	174	-3.9
		120	93	3.8	3.6	172	162	-6.0
		120	136	4.2	4.1	157	152	-3.5
		120	119	4.0	3.9	157	155	-1.3
		120	185	4.6	4.5	147	144	-2.0
		120	272	5.2	5.1	137	135	-1.5
		120	298	5.7	5.3	142	133	-6.4
		120	463	6.3	6.1	128	124	-3.4
		120	681	7.1	7.0	118	116	-1.8
A: S10C (annealed) (32)	Hole	120	632	7.1	6.8	123	117	-4.6
B: S30C (annealed) (39)	Notch	153	16	2.0	2.3	220	247	12.3
		153	16	2.1	2.3	225	247	9.9
		153	16	2.1	2.3	225	247	9.9
		153	32	2.6	2.8	199	220	10.7
		153	32	2.6	2.8	204	220	8.0
		153	32	2.7	2.8	208	220	5.5
		153	63	3.6	3.6	196	196	-0.2
		153	63	3.6	3.6	196	196	-0.2
		153	63	3.6	3.6	196	196	-0.2
		153	316	5.7	6.1	140	150	7.3
		153	316	5.7	6.1	140	150	7.3
		153	316	5.9	6.1	144	150	4.0
C: S35C (annealed) (40)	Notch	160	632	7.0	7.9	120	137	14.0
		160	632	7.1	7.9	122	137	12.4
		160	632	7.3	7.9	126	137	8.4
C: S35C (annealed) (41)	Notch	160	316	5.9	6.3	144	154	6.5
		160	474	6.4	7.2	127	144	13.1
		160	949	7.2	9.1	101	128	26.3
C: S35C (annealed) (27)	Hole	160	409	7.1	6.9	152	147	-3.2
		160	681	8.2	8.1	137	135	-1.3
D-1: S45C (annealed) (42)–(44)	Notch	180	16	2.6	2.5	280	271	-3.1
		180	16	2.5	2.5	275	271	-1.4
		180	16	2.5	2.5	275	271	-1.4
		180	32	3.2	3.1	245	242	-1.4
		180	32	3.2	3.1	250	242	-3.4
		180	32	3.2	3.1	245	242	-1.4
		180	316	6.6	6.7	160	165	2.9
		180	316	6.6	6.7	160	165	2.9
		180	316	6.2	6.7	151	165	8.9

Continued

Table 1 (Continued)

Material	Defect	H _v	√area (μm)	ΔK _{th} (MPa√m)		σ _w (MPa)		Error (%)
				Expt	Pred.	Expt	Pred.	
D-2: S45C (annealed) (20)(28)	Hole	170	37	3.3	3.2	235	228	-3.2
		170	46	3.5	3.4	226	219	-3.0
		170	68	4.3	3.9	226	206	-9.1
		170	48	3.7	3.5	230	218	-5.2
		170	74	4.2	4.0	211	203	-3.9
		170	109	4.8	4.6	201	190	-5.5
		170	60	4.0	3.7	226	210	-7.0
		170	60	4.0	3.7	226	210	-7.0
		170	93	4.5	4.3	201	195	-2.8
		170	93	4.3	4.3	196	195	-0.4
		170	136	5.1	4.9	191	183	-4.1
		170	119	5.1	4.7	201	187	-6.9
		170	185	5.7	5.5	181	174	-3.9
		170	272	6.5	6.2	172	163	-5.2
		170	298	7.2	6.4	181	161	-11.2
		170	463	7.8	7.4	157	149	-4.9
		170	681	8.8	8.4	147	140	-4.7
		E: S50C (annealed) (45)	Notch	177	316	5.9	6.7	144
177	316			5.9	6.7	144	163	13.2
E: S50C (annealed) (47)	Circumferential crack	177	95	4.4	4.5	196	199	1.5
		177	379	7.2	7.1	160	158	-1.2
		177	538	7.1	8.0	133	149	11.9
		177	791	8.0	9.1	123	140	13.5
F: S45C (quenched) (29)(30)	Hole	650	37	9.3	8.5	667	604	-9.4
		650	62	10.3	10.1	568	554	-2.5
		650	93	12.4	11.5	559	518	-7.4
		650	117	11.7	12.4	470	499	6.1
G: S45C (quenched and tempered) (29)(30)	Hole	520	37	8.0	7.0	568	502	-11.6
		520	62	9.4	8.4	519	460	-11.3
		520	117	10.5	10.3	421	414	-1.6
		520	202	12.5	12.4	382	378	-1.0
H: S50C (quenched and tempered) (45)	Notch	319	316	8.6	9.9	209	241	15.3
I-1: S50C (quenched and tempered) (45)	Notch	378	316	10.3	11.2	252	273	8.2

Continued

Table 1 (Continued)

Material	Defect	H _v	√area (μm)	ΔK _{th} (MPa√m)		σ _w (MPa)		Error (%)
				Expt	Pred.	Expt	Pred.	
I-2: S50C (quenched and tempered) (39)	Notch	375	16	4.3	4.1	468	447	-4.4
		375	16	4.4	4.1	478	447	-6.4
		375	63	6.8	6.5	373	355	-4.8
		375	63	6.8	6.5	373	355	-4.8
		375	316	10.3	11.1	252	272	7.6
		375	316	10.3	11.1	252	272	7.6
		375	316	10.3	11.1	252	272	7.6
J: 70/30 brass (46)	Notch	70	316	3.6	4.3	87	104	19.5
		70	316	3.6	4.3	87	104	19.5
J: 70/30 brass (33)	Hole	70	93	2.6	2.8	118	128	8.4
		70	185	3.4	3.6	108	114	5.6
		70	463	4.9	4.8	98	98	-0.3
K: Aluminum alloy (2017-T4) (33)	Hole	114	74	3.0	3.2	152	164	7.6
		114	93	3.3	3.5	147	158	7.2
		114	185	3.9	4.4	123	140	14.1
L: Stainless steel (SUS603) (34)	Hole	355	37	7.4	5.2	530	373	-29.7
		355	74	8.7	6.6	441	332	-24.7
		355	93	9.8	7.1	441	320	-27.5
		355	139	11.7	8.1	432	299	-30.8
		355	185	11.7	8.9	373	285	-23.6
M: Stainless steel (YUS170) (34)	Hole	244	93	6.7	5.4	304	245	-19.4
		244	139	8.0	6.2	294	229	-22.1
		244	185	8.3	6.8	265	218	-17.6
N: Maraging steel (35)	Vickers hardness indentation	720	19	6.9	7.4	686	736	7.3
	Hole	720	37	9.5	9.2	677	659	-2.7
		720	93	11.7	12.5	530	566	6.7
		720	185	13.8	15.8	441	504	14.3
	Notch	720	63	10.0	11.0	546	603	10.4
		720	95	10.2	12.6	454	563	24.0

S10C: ~0.10% carbon steel
 S30C: ~0.30% carbon steel
 S35C: ~0.35% carbon steel
 S45C: ~0.45% carbon steel
 S50C: ~0.50% carbon steel

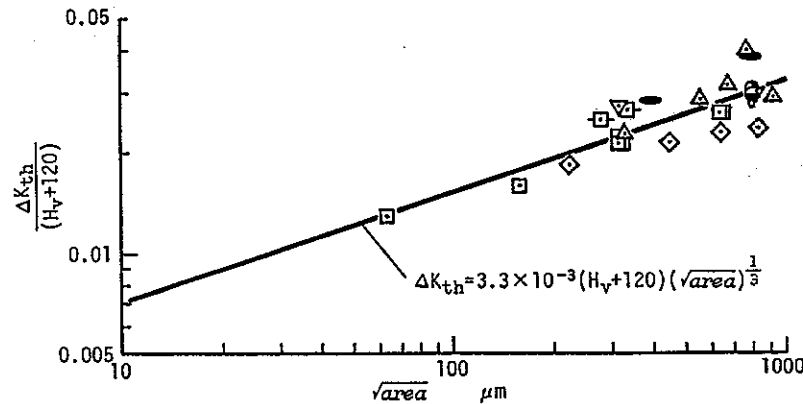


Fig 5 Relationship between $\Delta K_{th}/(H_v + 120)$ and \sqrt{area} . Most of the H_v values are estimated by equation (10). See Table 2 for symbol references

Applications

After obtaining equation (8), the data of other references (9)(47)(57)(58)–(64) were investigated. Few of them present the hardness of materials. Therefore, H_v was estimated by using the relationship between H_v and H_B (ASTM E-48-43-T) and an empirical formula which is thought to hold between ultimate tensile strength and H_B , i.e.

$$\sigma_U \cong 0.36(9.8 \times H_B) \quad (10)$$

Figure 5 and Table 2 provide details of the comparison between the prediction by equation (8) and the experimental data. Although these references lack the data for very small values of \sqrt{area} , it may be concluded that equation (8) predicts ΔK_{th} very well for cracked or notched specimens having \sqrt{area} less than 1000 μm .

Table 2 A collection of data from the different studies used in Fig. 5

Material	Defect	Researchers
● 0.12% C steel	Fatigue crack	Isibasi and Uryu (58)
● 0.53% C steel	Fatigue crack	Isibasi and Uryu (58)
△ SF60	Artificial crack	Ouchida and Kusumoto (59)
▽ Mild steel	Fatigue crack	Frost (9)
□ S20C	Circumferential notch	Nisitani (57)(61)
□ S20C	Drilled hole	Nisitani and Kage (60), Hayashi <i>et al.</i> (62)
○ S25C	Fatigue crack	Awatani and Matsunami (63)
● S35C	Fatigue crack	Kobayashi and Nakazawa (64)
◇ Eutectoid steel	Circumferential notch	Kobayashi and Nakazawa (47)

The limitation of the applicability of equations (8) and (9)

As seen in Fig. 4, equations (8) and (9) can be applied to small defects or cracks within some range of the value of \sqrt{area} . Although the upper limit of the size of \sqrt{area} for the application of these equations is uncertain at present, it may be approximately 1000 μm . The lower limit is dependent on material properties and microstructures. In experiments we have a finite value of the fatigue limit σ_w for specimens containing no defects or cracks. Theoretically, in this case, $\sqrt{area} = 0$ and accordingly $\sigma_w = \infty$. But this never occurs, because cracks along slip bands or grain boundaries nucleate as a result of reversed slip in grains, that is, \sqrt{area} is not zero, and accordingly the fatigue limit of defect-free specimens σ_{w_0} becomes finite. Therefore, as discussed in previous studies (28)–(30), the lower limit of \sqrt{area} for the application of equations (8) and (9) is related to the maximum length, l_0 , of non-propagating cracks observed in unnotched (defect-free) specimens. It follows that even if a specimen contains small defects or cracks before fatigue tests, and if the fatigue limit σ_w predicted from the value of \sqrt{area} and equation (9) is greater than σ_{w_0} , the value of σ_w is never measured because such defects do not lower the fatigue strength of the specimen and they are virtually harmless. When we know the value of σ_{w_0} in advance, the lower limit of \sqrt{area} can be determined from equation (9). When σ_{w_0} is unknown, its approximate value can be estimated by the empirical formula

$$\sigma_{w_0} \cong 0.5\sigma_U \cong 1.6H_v \quad (11)$$

where σ_U is the ultimate tensile strength in MPa. So far, it has been said that equation (11) is not necessarily applicable to high-strength or hard steels (65). However, such a conclusion was based on experiments in which the original site of fatigue fracture – whether it was slip bands or defects – was not identified exactly. Murakami and Endo (29)(30) showed on the basis of careful investigations of fracture origins that equation (11) is applicable to hard steels when defects are not the cause of fatigue fracture.

Concluding remarks

The dependence of ΔK_{th} on crack size and material properties was investigated on more than ten materials and microstructures. The value of ΔK_{th} of all materials were unified with one geometrical together with one material parameter.

The geometrical parameter is the square root of the area which is occupied by projecting the defects or cracks onto the plane normal to the maximum tensile stress. It was found that

$$\Delta K_{th} \propto (\sqrt{area})^{1/3}$$

The material parameter to unify data is the Vickers hardness value, H_v . The

influence of microstructural variables and the difference of materials can be unified by the following equation

$$\Delta K_{th} \propto (H_v + 120)$$

The constant of 120 in the above equation reflects the experimental fact that relatively large non-propagating cracks are likely to be observed in low strength metals in comparison with hard metals. Combining the above two equations, we find by experiment that

$$\Delta K_{th} = 3.3 \times 10^{-3} (H_v + 120) (\sqrt{area})^{1/3}$$

for threshold stress intensity factor ranges at a stress ratio, R , equal to -1 , and

$$\sigma_w = 1.43 (H_v + 120) / (\sqrt{area})^{1/6}$$

for the fatigue limit, where the units of the quantities in these equations are $MPa\sqrt{m}$ for ΔK_{th} , MPa for σ_w , and μm for \sqrt{area} .

Although the upper limit of \sqrt{area} for the application of the above equations is uncertain at present, it may be approximately $1000 \mu m$. The lower limit can be estimated from the fatigue strength of unnotched (defect-free) specimens or from the length of the maximum non-propagating crack which is observed at the fatigue limit of an unnotched specimen.

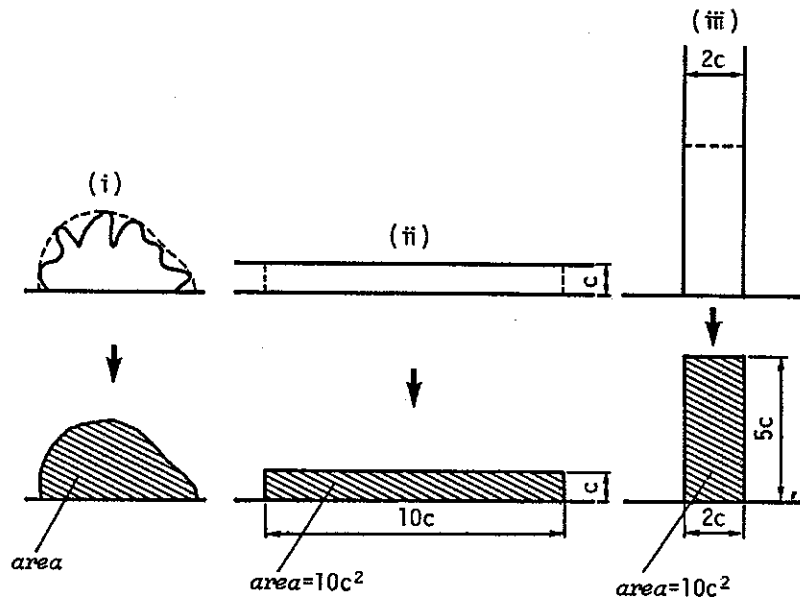


Fig 6

Appendices

Appendix 1

Figure 6 gives rules for the estimation of \sqrt{area} for irregularly shaped cracks and very slender cracks (24) (25). (See also (20) (66).)

The long shallow and very deep cracks shown in Fig. 6 as (ii) and (iii), respectively, must be bounded by a maximum length of $10c$ and $5c$, respectively, for the estimation of effective crack area.

Appendix 2

Figure 7 shows the relationship between the maximum stress intensity factor $K_{I\max}$ and \sqrt{area} for surface cracks (elastic analysis) (24)(25). (See also (20)(66).)

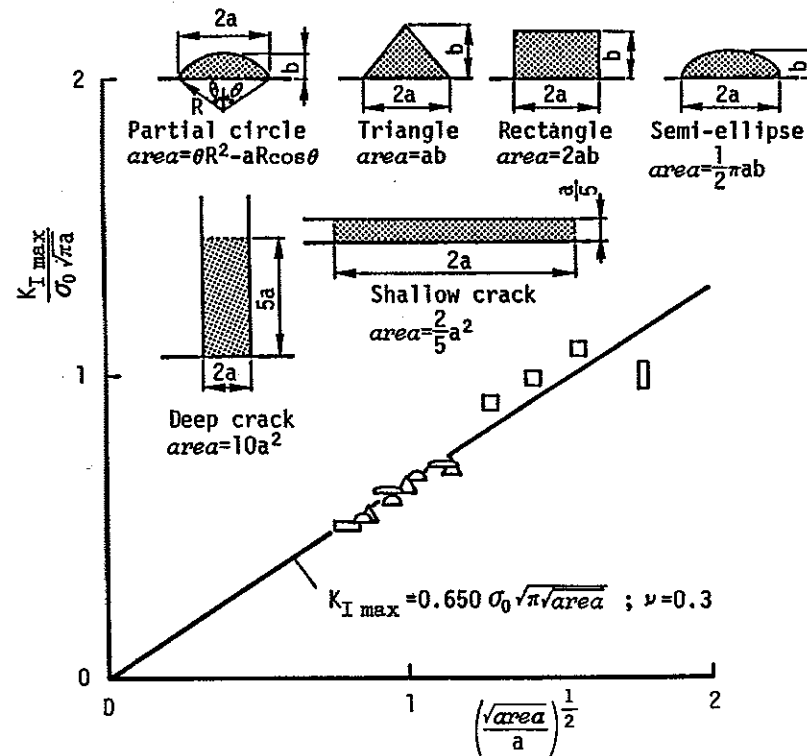


Fig 7

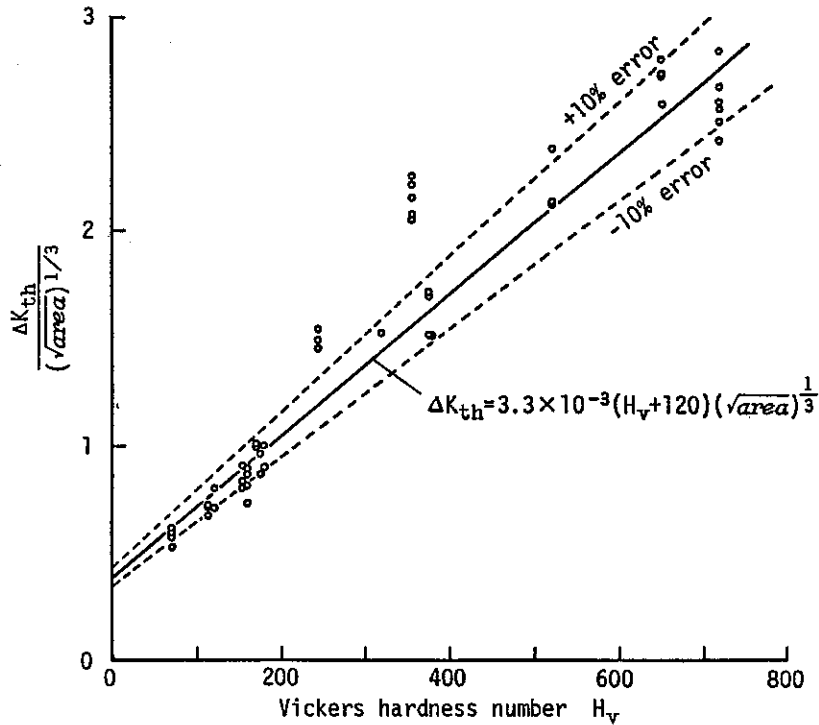


Fig 8

Appendix 3

Figure 8 shows the dependence of $\Delta K_{th}/(\sqrt{area})^{1/3}$ on the material parameter (H_V) for various materials.

References

- (1) FROST, N. E., POOK, L. P., and DENTON, K. (1971) A fracture mechanics analysis of fatigue crack growth data for various materials, *Engng. Fracture Mech.*, **3**, 109–126.
- (2) KOBAYASHI, H. and NAKAZAWA, H. (1972) A stress criterion for fatigue crack propagation in metals, *Proc. 1st Int. Conf. Mech. Behavior Mater.*, Kyoto, Japan, pp. 199–208.
- (3) KITAGAWA, H. and TAKAHASHI, S. (1976) Applicability of fracture mechanics to very small cracks or the cracks in the early stage, *Proc. 2nd Int. Conf. Mech. Behavior Mater.*, Boston, USA, pp. 627–631.
- (4) ROMANOV, O. N., SIMINKOVICH, V. N., and TKACK, A. N. (1981) Near-threshold short fatigue crack growth, *Fatigue Thresholds: Fundamentals and Engineering Applications*, Vol. II (Edited by Bäcklund, J., Blom, A. F., and Beevers, C. J.), pp. 799–807.
- (5) LIES, B. N., KANNINEN, M. F., HOPPER, A. T., AHMAD, J., and BREOK, D. (1983) A critical review of the short fatigue crack in fatigue, Battelle's Columbus Laboratories, Report No. AFWAL-TR-83-4019, pp. 1–135.
- (6) SURESH, S. and RITCHIE, R. O. (1983) The propagation of short fatigue cracks, Report No. UCB/RP/83/1014, pp. 1–70.
- (7) KIKUKAWA, M., JONO, M., TANAKA, K., and TAKATANI, M. (1976) Measurement of fatigue crack propagation and crack closure at low stress intensity level by unloading elastic compliance method, *J. Soc. Mater. Sci. Japan*, **25**, 899–903.
- (8) BYRNE, J. and DUGGAN, T. V. (1981) Near-threshold short fatigue crack growth, *Fatigue Thresholds: Fundamentals and Engineering Applications*, Vol. II (Edited by Bäcklund, J., Blom, A. F., and Beevers, C. J.), pp. 759–775.
- (9) FROST, N. E. (1959) A relation between the critical alternating propagation stress and crack length for mild steel, *Proc. Instn mech. Engrs*, **173**, 811–835.
- (10) EL HADDAD, M. H., SMITH, K. N., and TOPPER, T. H. (1979) Fatigue crack propagation of short cracks, *Trans Am. Soc. Test. Mater.*, **101**, 42–46.
- (11) CUMMINGS, H. N., STULEN, F. B., and SCHULTE, W. C. (1958) Tentative fatigue strength reduction factors for silicate-type inclusions in high-strength steels, *Proc. Am. Soc. Test. Mater.*, **58**, 505–514.
- (12) FUJIWARA, T. and FUKUI, S. (1964) The effect of non-metallic inclusions on the fatigue life of ball-bearing steel, *Electr. Furnace Steel*, **35**, 170–177.
- (13) RAMSEY, P. W. and KEDZIE, D. P. (1957) Prot fatigue study of an aircraft steel in the ultra high strength range, *J. Metals*, 401–407.
- (14) HYLER, W. S., TARASOV, L. P., and FAVOR, R. J. (1958) Distribution of fatigue failures in flat hardened steel test bars, *Proc. Am. Soc. Test. Mater.*, **58**, 540–551.
- (15) JOHNSON, R. F. and SEWELL, J. F. (1960) The bearing properties of 1% C-Cr steel as influenced by steelmaking practice, *J. Iron Steel Inst.*, **196**, 414–444.
- (16) DUCKWORTH, W. E. and INESON, E. (1963) The effects of externally introduced alumina particles on the fatigue life of En24 steel, *Iron Steel Inst. Sp. Rep.*, **77**, 87–103.
- (17) KAWADA, Y., NAKAZAWA, H., and KODAMA, S. (1963) The effects of the shapes and the distributions of inclusions on the fatigue strength of bearing steels in rotary bending, *Trans Japan Soc. mech. Engrs*, **29**, 1674–1683.
- (18) UHRUS, L. O. (1963) Through-hardening steels for ball bearings – effect of inclusions on endurance, *Iron Steel Inst. Sp. Rep.*, **77**, 104–109.
- (19) DE KAZINCZY, F. (1970) Effect of small defects on the fatigue properties of medium-strength cast steel, *J. Iron Steel Inst.*, **208**, 851–855.
- (20) MURAKAMI, Y. and ENDO, M. (1983) Quantitative evaluation of fatigue strength of metals containing various small defects or cracks, *Engng Fracture Mech.*, **17**, 1–15.
- (21) HAMMOUDA, M. M. and MILLER, K. J. (1979) Elastic-plastic fracture mechanics analyses of notches, *ASTM STP 668*, pp. 703–719.
- (22) SMITH, R. A. and MILLER, K. J. (1978) Prediction of fatigue regimes in notched components, *Int. J. Mech. Sci.*, **20**, 201–206.
- (23) MURAKAMI, Y. and NEMAT-NASSER, S. (1983) Growth and stability of interacting surface flaws of arbitrary shape, *Engng Fracture Mech.*, **17**, 193–210.
- (24) MURAKAMI, Y. and ISIDA, M. (1985) Analysis of an arbitrarily shaped surface crack and stress field at crack front near surface, *Trans Japan Soc. mech. Engrs*, **51**, 1050–1056.
- (25) MURAKAMI, Y. (1985) Analysis of stress intensity factors of modes I, II and III for inclined surface cracks of arbitrary shape, *Engng Fracture Mech.*, **22**, 101–114.
- (26) NISITANI, H. and MURAKAMI, Y. (1973) Effect of spheroidal graphite on bending and torsional fatigue strength of nodular cast iron, *Science of Machines*, **25**, 543–546.
- (27) NISITANI, H. and KAWANO, K. (1971) Correlation between the fatigue limit of a material with defects and its non-propagating crack: some considerations based on the bending or torsional fatigue of the specimen with a diametrical hole, *Trans Japan Soc. mech. Engrs*, **37**, 1492–1496.
- (28) MURAKAMI, Y. and ENDO, T. (1980) Effects of small defects on fatigue strength of metals, *Int. J. Fatigue*, **2**, 23–30.
- (29) MURAKAMI, Y. and ENDO, T. (1981) The effects of small defects on the fatigue strength of hard steels, *Fatigue 81* (Warwick University, UK), pp. 431–440.

- (30) MURAKAMI, Y., KAWANO, H., and ENDO, T. (1979) Effect of micro-holes of fatigue strength (the 2nd report: effect of micro-holes of 40 μm –200 μm in diameter on the fatigue strength of quenched or quenched and tempered 0.46% carbon steel), *Trans Japan Soc. mech. Engrs*, **45**, 1479–1489.
- (31) MURAKAMI, Y. (1984) Size effect of ΔK_{th} : ΔK_{th} of small surface cracks as the function of crack area, *Prelim. Proc. 61st Annual Meeting of Japan Soc. Mech. Engrs*. No. 840–2, pp. 1–3.
- (32) NISITANI, H. and KAGE, M. (1973) Rotating bending fatigue of electropolished specimens with transverse holes – observation of slip bands and non-propagating cracks near the holes, *Trans Japan Soc. mech. Engrs*, **39**, 2005–2012.
- (33) MURAKAMI, Y., TAZUNOKI, Y., and ENDO, T. (1984) Existence of the coaxing effect and effects of small artificial holes on fatigue strength of an aluminum alloy and 70–30 brass, *Metall. Trans.*, **15A**, 2029–2038.
- (34) NISHIDA, S. (1985) private communication.
- (35) MURAKAMI, Y., KIYOTA, T., ENOMOTO, K., and ABE, M. (1985) Effects of artificial small defects on the fatigue strength of a maraging steel, *Prelim. Proc. 34th Annual Meeting of the Soc. Mater. Sci. Japan*, pp. 148–150.
- (36) OBA, H., MURAKAMI, Y., and ENDO, T. (1983) Effects of artificial small holes on fatigue strength of notched specimens, *Trans Japan Soc. mech. Engrs*, **49**, 901–910.
- (37) NISITANI, H. and NISHIDA, S. (1970) Change in surface states and incipient fatigue cracks in electro-polished low carbon steel (plain and notched specimens) under rotating bending stress, *Bull. Japan Soc. mech. Engrs*, **13**, 961–967.
- (38) NISITANI, H. and MURAKAMI, Y. (1969) Torsional fatigue and bending fatigue of electropolished low carbon steel specimens, *Bull. Japan Soc. mech. Engrs*, **13**, 325–333.
- (39) NISITANI, H. (1972) Correlation between notch sensitivity of a material and its non-propagating crack, under rotating bending stress, *Proc. 1st Int. Conf. Mech. Behavior of Mater.*, Kyoto, Japan, pp. 312–322.
- (40) NISITANI, H. and KAWANO, K. (1968) Non-propagating crack and crack strength of shafts with a shoulder fillet subjected to rotary bending, *Proc. 11th Japan Congr. Mater. Research – Metallic Mater.*, Japan, pp. 49–51.
- (41) KOBAYASHI, H. and NAKAZAWA, H. (1969) The effects of notch depth on the initiation, propagation and non-propagation of fatigue cracks, *Trans Japan Soc. mech. Engrs*, **35**, 1856–1863.
- (42) NISITANI, H. and ENDO, M. (1985) Fatigue strength of carbon steel specimens having an extremely shallow notch, *Engng Fracture Mech.*, **21**, 215–227.
- (43) NISITANI, H. and ENDO, M. (1985) Unifying treatment of notch effects in fatigue, *Trans Japan Soc. mech. Engrs*, **51**, 784–789.
- (44) NISITANI, H. and ENDO, M. (1984) Unified treatment of deep and shallow notches in rotating bending fatigue, *ASTM STP*, submitted for publication.
- (45) NISITANI, H. and CHISHIRO, I. (1974) Non-propagating micro-cracks of plain specimens and fatigue notch sensitivity in annealed or heat-treated 0.5% C steel, *Trans Japan Soc. mech. Engrs*, **40**, 41–52.
- (46) NISITANI, H. and OKAZAKA, K. (1973) Effect of mean stress on fatigue strength, crack strength and notch radius at branch point under repeated axial stress, *Trans Japan Soc. mech. Engrs*, **39**, 49–59.
- (47) KOBAYASHI, H. and NAKAZAWA, H. (1970) On the alternating stress required to propagate a fatigue crack in carbon steel (continued report), *Trans Japan Soc. mech. Engrs*, **36**, 1789–1798.
- (48) MURAKAMI, Y. and MATSUDA, K., in preparation.
- (49) ISIBASI, T. (1960) Fatigue strength of notched stainless steel specimens, *Proc. 3rd Japan Congr. Test Mater.*, Japan, pp. 24–26.
- (50) OUCHIDA, H. and ANDO, S. (1964) The fatigue strength of notched specimens at low temperatures, *Trans. Japan Soc. mech. Engrs*, **30**, 52–58.
- (51) OGURA, K., MIYOSHI, Y., and NISHIKAWA, I. (1983) Fatigue crack growth and closure at notch root of SUS304 stainless steel, *Proc. 26th Japan Congr. Mater. Research – Metallic Mater.*, Japan, pp. 91–96.
- (52) KAWAI, S. and KASAI, K. (1985) Considerations of allowable stress of corrosion fatigue (focused on the influence of pitting), *Fatigue Fracture Engng Mater. Structures*, **8**, 115–127.

- (53) ISIBASI, T. (1948) On the fatigue limits of notched specimens, *Memo. Fac. Engng. Kyushu University*, **11**, 1–31.
- (54) PETERSON, R. E. (1953) *Stress Concentration Design Factors* (John Wiley, New York), p. 8.
- (55) SIEBEL, E. and STIELER, M. (1955) Ungleichförmige spannungsverteilung bei schwingender beanspruchung, *Zeitschrift VDI*, **97**, 121–126.
- (56) HEYWOOD, R. B. (1962) *Designing against fatigue* (Chapman & Hall, London), p. 95.
- (57) NISITANI, H. (1968) Effects of size on the fatigue limit and the branch point in rotary bending tests of carbon steel specimens, *Bull. Japan Soc. mech. Engrs*, **11**, 947–957.
- (58) ISIBASI, T. and URYU, T. (1953) Fatigue strength of carbon steel bars with round-crack, *Rep. Res. Inst. Appl. Mech.*, *Kyushu University*, **2**, 65–74.
- (59) OUCHIDA, H. and KUSUMOTO, S. (1954) Fatigue strength of carbon steel bars with artificial cracks, *Trans Japan Soc. mech. Engrs*, **20**, 739–745.
- (60) NISITANI, H. and KAGE, M. (1977) Effect of annealing or change in stress level on the condition for propagation of non-propagating fatigue cracks, *Trans Japan Soc. mech. Engrs*, **43**, 398–406.
- (61) NISITANI, H. (1968) *Prelim. Proc. 46th Annual Meeting Japan Soc. Mech. Engrs*, Japan, No. 198, pp. 37–40.
- (62) HAYASHI, I., SUZUKI, T., and MORITA, J. (1982) Mechanism of non-propagating crack of notched low carbon steel specimen near the stage of rotating bending fatigue limit, *Proc. 25th Japan Congr. Mater. Research – Metallic Mater.*, Japan, pp. 80–86.
- (63) AWATANI, J. and MATSUNAMI, K. (1977) On non-propagating fatigue cracks in specimens with cracks, *J. Soc. Mater. Sci. Japan*, **26**, 343–347.
- (64) KOBAYASHI, H. and NAKAZAWA, H. (1967) On the alternating stress required to propagate a fatigue crack in carbon steels, *Trans Japan Soc. mech. Engrs*, **33**, 1529–1534.
- (65) GARWOOD, M. F., ZURBERG, H. H., and ERIKSON, M. A. (1951) Correlation of laboratory test and service performance. *Interpretation of tests and correlation with service* (American Society of Metals), pp. 1–77.
- (66) ENDO, M. and MURAKAMI, Y. (1985) Fatigue strength of defect and cracked materials – discussion based on the crack area, *Prelim. 38th Annual Meeting of Japan Soc. Mech. Engrs. Kyushu*, Japan, No. 858–1, pp. 63–65.